Journal of Sound and Vibration (1999) **227**(5), 979–986
Article No. jsvi.1999.2590, available online at http://www.idealibrary.com on IDEAL®

POLYGONALIZATION OF WHEEL TREADS CAUSED BY STATIC AND DYNAMIC IMBALANCES*

P. MEINKE
TU Berlin and Uni Stuttgart,
AND
S. MEINKE
I.A.T. mbH, *Gautingerstr*. 7*a*, *D*-92319 *Starnberg*, *Germany*

(*Accepted* 18 *January* 1999)

High speed wheelsets of railway systems differ from classical ones. There dynamics are determined by gyroscopic and inertia moments. A dynamical model with 40-DOF was generated using elastic beam elements to describe the axle, connected to rigid wheel and brake disks. Imbalance calculations and wear simulations were carried out resulting in polygonalization of the circular wheel surface. Even when starting the simulation with wheels of constant radius, the unroundness grows to unacceptable values.

1. INTRODUCTION

The dynamic behaviour of wheelsets of modern high speed trains differs from that of "classical" wheelsets for two reasons.

First, due to increased kinetic energy of the high speed trains more braking power is necessary. Therefore, these wheelsets are equipped with more braking disks than usual, typically with four instead of two disks.

Second, as the diameter of the high speed wheelsets is similar to that of lower speed wheels of the same railway company, the rotational speed of the former wheelsets is substantially higher than usual.

By calculation it has been proven that the effects of rotary inertia and gyroscopic moments dominate vibrations of the high speed wheelsets, in contrary to the standard wheelsets. In other words, the high speed wheelsets vibrations are a matter of rotor dynamics and are governed by gravitational, gyroscopic and inertia forces [1, p.233], [2, p.272].

The differential equation of these wheelsets (see Figure 1), modelled as an elastic multi-body system (see Figure 2), are generated by application of the

*Dedicated to Prof. Dr. Roman. Bogacz and to Prof. Dr.-Ing. Klaus Knothe on occasion of their 60th birthdays.

0022–460X/99/450979 + 08 $30.00/0

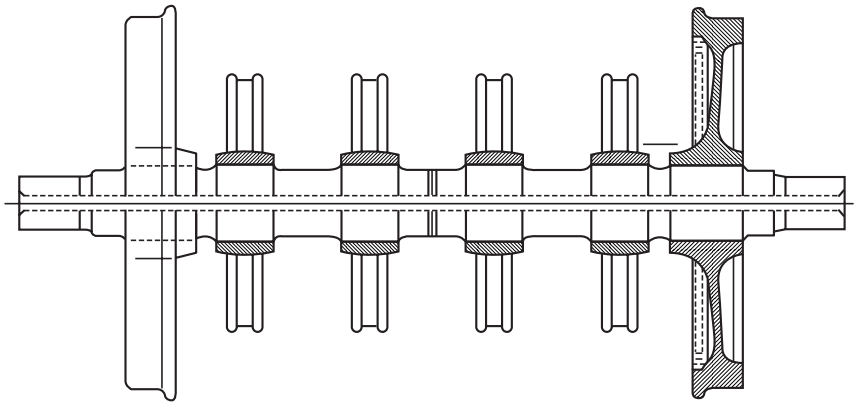

Figure 1. High speed wheelset.

impulse and angular momentum laws [3] and is deduced in reference [1, p. 238ff] (including imbalances): It is

$$[\mathbf{MS} + \mathbf{MR}]\underline{\ddot{\mathbf{x}}} + [\mathbf{D} + \mathbf{G}]\underline{\dot{\mathbf{x}}} + [\mathbf{CS} + \mathbf{N}]\underline{\mathbf{x}} = \underline{\mathbf{F}}(\Omega, t). \tag{1}$$

Here **MS** is the modal mass matrix of the shaft elements, **MR** is the mass matrix of the rotor/disc elements, **D** is the damping matrix = α**MS** + β**CS**, **G** is the gyroscopic matrix, **CS** is the modal spring matrix of the shaft elements and the suspensions, **N** is the matrix of non-conservative effects, $\underline{\mathbf{F}}$ is the excitation vector due to imbalance and track irregularities, Ω is the rotational frequency of the wheelset and $\underline{\mathbf{x}}$ is the state vector. The static imbalance $\underline{a}^i$ is

$$\underline{a}^i = \begin{pmatrix} a_1^i \\ a_2^i \\ 0 \end{pmatrix},$$

and the inertial tensor J_{kl}^i is (including dynamic imbalance)

$$J_{kl}^i = \begin{pmatrix} A^i & -F^i & -E^i \\ -F^i & B^i & -D^i \\ -E^i & -D^i & C^i \end{pmatrix}.$$

2. DYNAMICS AT ROTATIONAL SPEED Ω, IMBALANCE RESPONSE

The manufactured wheelsets contain small inaccuracies, static and dynamic imbalances. The imbalance response, e.g., the passing of critical speeds, has to be considered. A cyclic response might be generally assumed. But in reality the vertical stiffness of the track is not necessarily equal to the longitudinal primary suspension of the wheelset. If one understands the wheelset as a spring–supported rotor, one has to use therefore an ansatz function, which is assumed with different amplitudes in the vertical and longitudinal directions:

$$\underline{\mathbf{x}}_i(t) = \underline{\mathbf{x}}_{ic} \cos \Omega t + \underline{\mathbf{x}}_{is} \sin \Omega t. \tag{2}$$

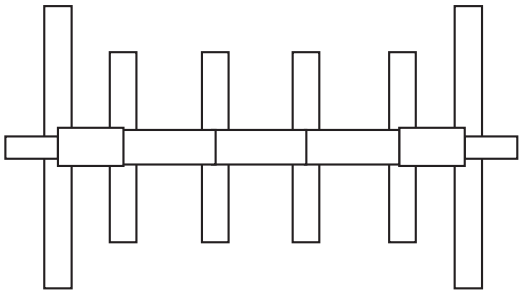

Figure 2. Dynamical model of the wheelset.

Upon using equation (2) equation (1) becomes

$$-\Omega^2 \underline{\underline{M}}_{ges} \underline{\mathbf{x}}_{ic} + \Omega \underline{\underline{D}}_{ges} \underline{\mathbf{x}}_{is} + \underline{\underline{C}}_{ges} \mathbf{x}_{ic} = \underline{F}_C, \quad -\Omega^2 \underline{\underline{M}}_{ges} x_{is} - \Omega \underline{\underline{D}}_{ges} x_{ic} + \underline{\underline{C}}_{ges} x_{is} = \underline{F}_S, \tag{3}$$

or, written as a matrix,

$$\begin{pmatrix} \underline{\underline{C}}_{ges} - \Omega^2 \underline{\underline{M}}_{ges} & \Omega \underline{\underline{D}}_{ges} \\ -\Omega \underline{\underline{D}}_{ges} & \underline{\underline{C}}_{ges} - \Omega^2 \underline{\underline{M}}_{ges} \end{pmatrix} \begin{pmatrix} \underline{q}_C \\ \underline{q}_S \end{pmatrix} = \begin{pmatrix} \underline{F}_C \\ \underline{F}_S \end{pmatrix}, \tag{4}$$

in which q_C represents the longitudinal component and q_S the vertical component of the stationary (elliptic) motion of the nodes.

Equation (4) produces an algebraic system of equations

$$\mathbf{U}\underline{\mathbf{Q}} = \mathbf{F}\underline{\mathbf{u}},$$

which can be solved by LU decomposition [4].

The FORTRAN 77 - code UNWUCHT has been used to compute the results shown in Figures 3 and 4, using input - data very similar to that of reference [5]. At low speeds the rotating wheelset vibrates in longitudinal direction, passing the critical speed of the primary suspension at about 10 Hz. Clearly visible is the anisotropic behaviour, because the amplitudes are different in longitudinal respectively vertical direction. The elliptic movement starts at about 100 km/h and is at the (unrealistic high) speed of approximately 900 km/h dominated by vertical components at 95 Hz.

For better illustration of the whole wheelset dynamics, of the two Figures 3 and 4, one is with solely static imbalance distribution at the disks of the wheelset [1, see Figure 9], and the other is with pure dynamic imbalances distributed at the four brake disks and at the two wheel disks: In the static imbalance case the wheels are ''calm'' compared with the brake disks. In the other case (dynamic imbalance) the wheels are ''violent'' in the comparison with the brakes.

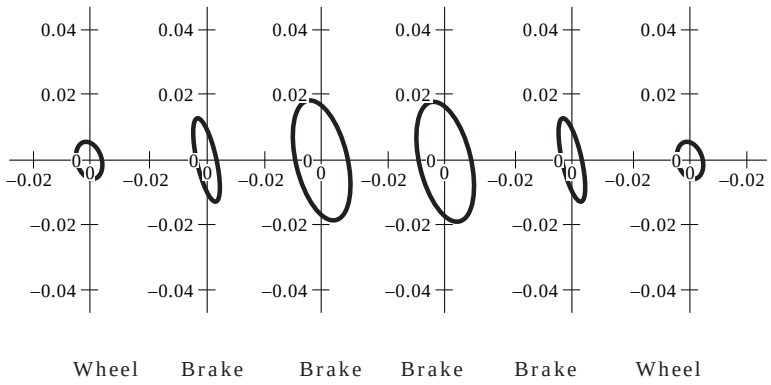

Figure 3. Stationary solution of an imbalanced–excited wheelset vibration (static imbalance at each wheel and brake disk).

3. WEAR AT THE SURFACES OF HIGH SPEED WHEELSETS, CAUSED BY IMBALANCE

The imbalance causes wear due to the short term dynamic behaviour, which creates creepage and polygonalization of the wheel surface in the "long term" behaviour. The mechanism of "self-excitation" is described in Figure 5 [1, see Figure 3).

By analyzing equation (1) a coupling between bending and torsional (ε) vibration can be discovered (longitudinal x_i, rotation around x_i, Φ_i; vertical z_i, rotation around z_i, Θ):

symmetrical at the mass matrix with

$$z_i,\ m_i a_1^i \cos(\Omega t) - m_i a_2^i \sin(\Omega t), \quad \Phi_i,\ -E_i \cos(\Omega t) + D_i \sin(\Omega t),$$

$$x_i,\ -m_i a_2^i \sin(\Omega t) - m_i a_2^i \cos(\Omega t), \quad \Theta_i,\ -E_i \sin(\Omega t) - D_i \cos(\Omega t);$$

unsymmetrical at the gyroscopic matrix with

$$z_i,\ 2m_i\,\Omega(a_1^i \sin(\Omega t) - m_i\, a_2^i \cos(\Omega t)), \quad \Phi_i,\ 2\Omega(E_i \sin(\Omega t) + D_i \cos(\Omega t)),$$

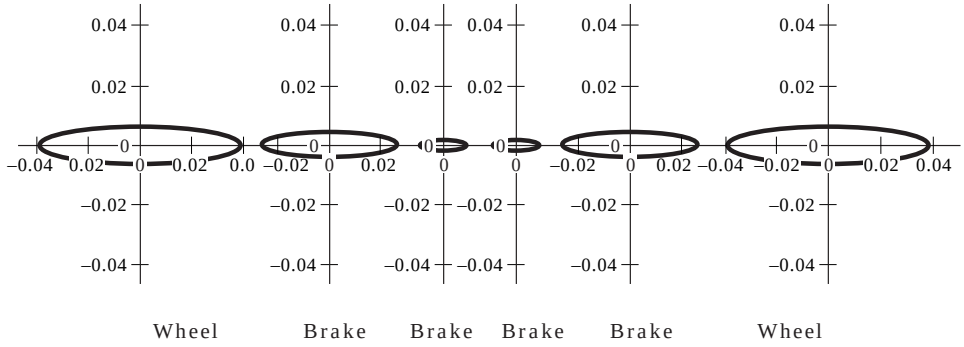

Figure 4. Stationary solution of an imbalanced–excited wheelset vibration (dynamic imbalance at each wheel and brake disc).

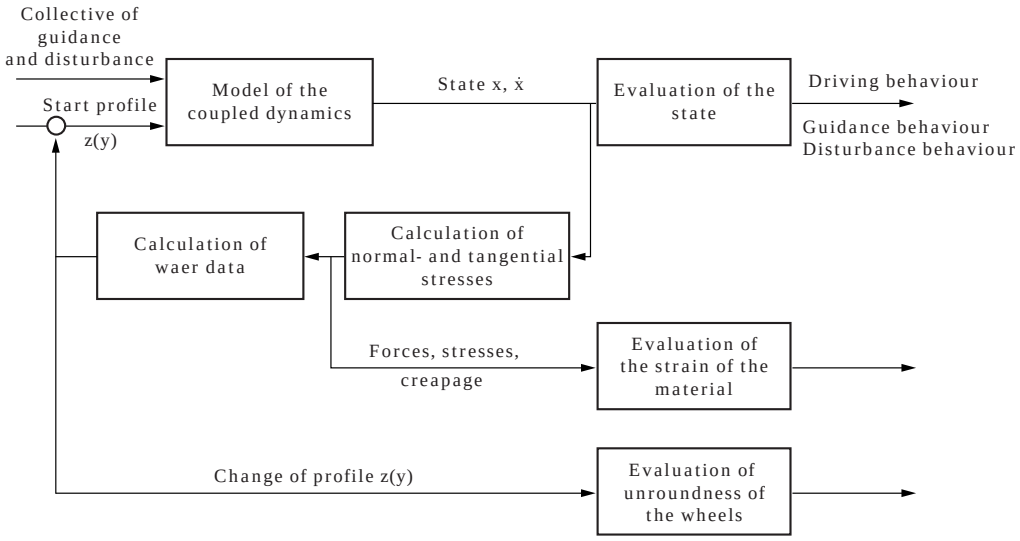

Figure 5. Interaction scheme of the short-term dynamics and the long-term behaviour.

$$x_i,\ 2m_i\,\Omega(-a_1^i\cos(\Omega t)+m_i\,a_2^i\sin(\Omega t)),\quad \Theta_i,\ 2\Omega(-E_i\cos(\Omega t)+D_i\sin(\Omega t));$$

antisymmetric at the spring matrix with

$$z_i,\ -m_i\Omega^2(-a_1^i\cos(\Omega t)+a_2^i\sin(\Omega t)),\quad \Phi_i,\ \Omega^2(E_i\cos(\Omega t)-D_i\sin(\Omega t)),$$

$$x_i,\ m_i\Omega^2(a_1^i\sin(\Omega t)+a_2^i\cos(\Omega t)),\quad \Theta_i,\ \Omega^2(E_i\sin(\Omega t)+D_i\cos(\Omega t)).$$

The bending/torsion–coupling occurs, as it is presented, in the presence of static as well as of dynamic imbalance.

By writing the state vector $\mathbf{w}$ as

$$\mathbf{w}=[x_i/\dot{x}_i], \tag{5}$$

the differential equation (1) can be formulated as the first order equation

$$\dot{\mathbf{w}}=\mathbf{B}\mathbf{w}+\mathbf{h}(t), \tag{6}$$

with

$$\mathbf{B}=\begin{bmatrix}\mathbf{0} & \mathbf{I}_{40}\\ -\mathbf{M}^{-1}\mathbf{Q} & -\mathbf{M}^{-1}\mathbf{P}\end{bmatrix},\quad \mathbf{h}=\begin{bmatrix}\mathbf{0}\\ \mathbf{M}^{-1}\mathbf{F}\end{bmatrix}. \tag{6a}$$

$\mathbf{B}$ is a 80×80 matrix and $\mathbf{I}_{40}$ the (40×40) identity matrix.

The force/creepage relation of the chosen wheel/rail model without lateral movement and without spin can be described by the points $P_1=(0,\ 0)$ and $P_2=(0{\cdot}01,\ \mu N)$, P_2 with horizontal tangent.

The FORTRAN 77 code UNRUND simulates the dynamics of the imbalanced–loaded rotating wheelset, running on the railheads with spring and

damper as suspension and it uses the subroutine DOBRI5 as a Runge–Kutta integrator.

The local wear in the surface of the wheel is described by the assumption

$$a = k_v W_R \tag{7}$$

where a is the local material loss by wear (mm), k_v is a coefficient (mm/Watt) and W_R is the friction energy (Watt s). The value of k_v is assumed to be 0·00005 kg/Joule, related to the contact area. This means with an estimated contact area of 1 cm^2 a specific material loss of 0·06 mm/Joule. The effective surface wear is due to sinusoidal movement of the wheelset less than estimated above. But on the other hand it is not possible to simulate many thousands of wheel revolutions. Therefore the values chosen for k_v are much bigger than physically necessary and the distances which the wheelset travels have to be extended by the ratio between the physical k_v and the chosen value of k_v.

The development of the radius $R(\varphi)$ of the wheel surface is

$$R(\varphi) = R(\varphi - 2\pi) - k_v W_R(\varphi). \tag{8}$$

The friction energy can be calculated by ($t_2 - t_1 = \Delta t$, where Δt is the integration step):

$$W_R = \int_{t_1}^{t_2} P_r \, \Delta t. \tag{9}$$

The friction power is

$$P_r = \mu(v) v(\varphi) v N(\varphi), \tag{10}$$

where $\mu(v)$ is the friction coefficient, dependent on creepage, $v(\varphi)$ is the creepage, dependent on the angle φ, v is the speed of the wheelset and $N(\varphi)$ is the normal force at the contact point, dependent on the angle φ.

Figure 6 shows the simulated development of an unround wheel surface under the load of dynamic imbalance during the first evolutions.

Usually unroundnesses are described by the Fourier coefficients of the quasistationary evolvable wheel circumference, which are practically periodic:

$$\begin{aligned} R(\varphi) = a_0 + a_1 \cos\varphi + a_2 \cos 2\varphi + \cdots + a_q \cos q\varphi \\ + b_1 \sin\varphi + b_2 \sin 2\varphi + \cdots + b_q \sin q\varphi. \end{aligned}$$

In UNRUND only the coefficients of the "spectral density" c_i are calculated:

$$c_i = \sqrt{(a_i^2 + b_i^2)}.$$

When using the known procedures (e.g. FFT) it is appropriate to divide the circumference into 2^n sections. In this example $16384 = 2^{14}$ sections have been chosen. This comparatively high number is used because the subroutine DOBRI5 needs small integration steps for a stable operation, and on the other hand the creepage calculation of the next revolution of the wheel ($\varphi + 2\pi$) needs the actual wheel diameter $R(\varphi)$. Figure 7 demonstrates the development of the

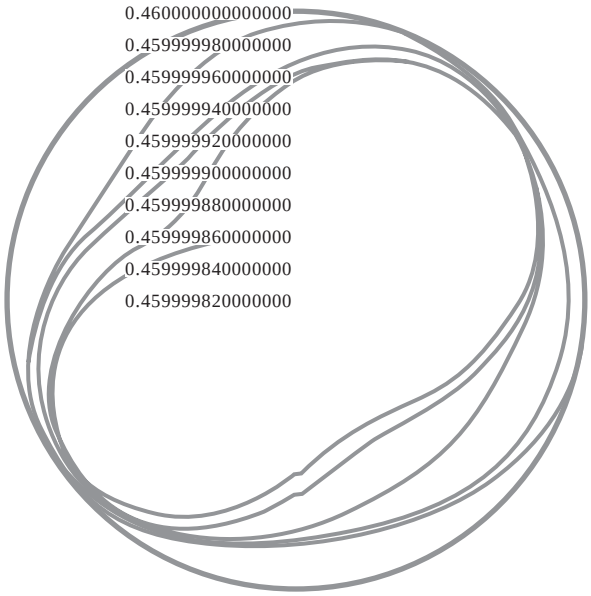

Figure 6. Development of unroundness of a originally cyclic wheel due to dynamic imbalance distributed over the wheelset.

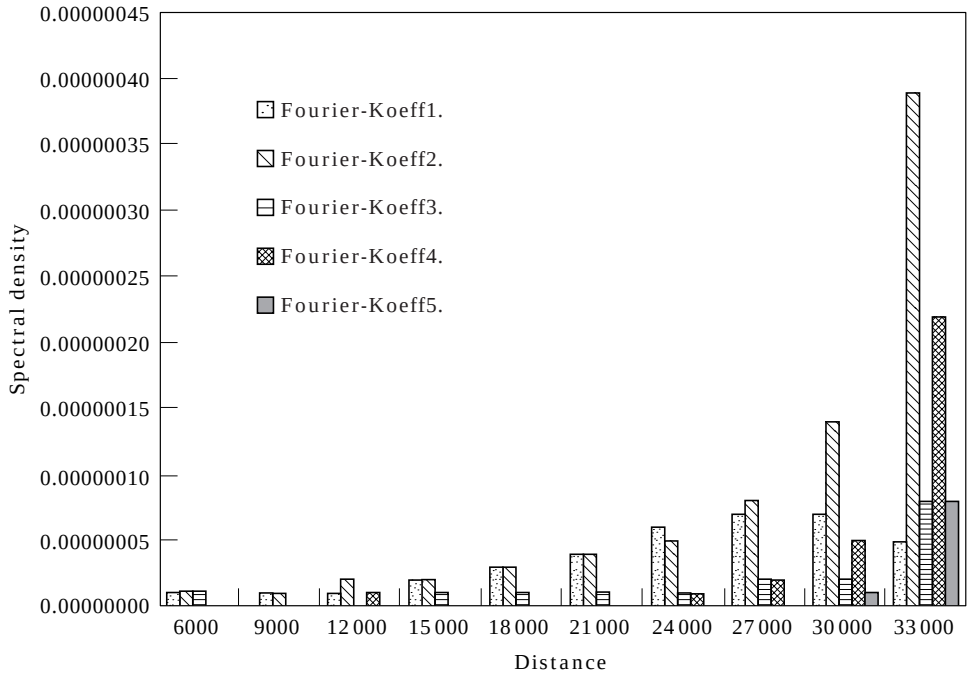

Figure 7. Development of polygonalization of the left wheel, described by spectral density coefficients. Fourier coefficients: Fourier coefficients: ⬚, 1; □, 2; □, 3; □, 4; ■, 5.

spectral density of polygonalisation during high speed operation of the unbalanced wheelset.

As a conclusion one has to conceive that the high speed wheelset is a rotor, of which the bearing matching consists of the wheel treads, running at the rails. This type of bearing is a trundling roller bearing. The material and the surface of these ''wheel/rail–bearings'' is not particularly good and wear, as trundling rolling is sensitive to wear due to creepage and creepage exists in any case between wheel and rail. If the creepage is invariable within time and phase angle, polygonalization of the wheel grows together with its unpleasant features.

REFERENCES

1. P. MEINKE, S. MEINKE and T. SZOLC 1996 4*th German - Polish Workshop on Dynamical Problems in Mechanical Systems*, *Warzawa*. On dynamics of rotating wheel/rail systems in a medium frequency range.
2. K. POPP and W. SCHIEHLEN 1993 B.G. Teubner. Stuttgart. *Fahrzeugdynamik*.
3. G. SCHWEITZER and W. SCHIEHLEN 1972 *Ingenieurarchiv* **41** 110–140. Kreiselverhalten eines elastisch gelagerten Rotors.
4. W. H. PRESS, S. A. TEUKOLSKI, W. T. Vetterling and B. P. FLANNERY 1986 *Numerical Recipes in Fortran*, *The Art of Scientific Computing*: Cambridge University Press.
5. H. CLAUS, I. KAISER, M. KÜSEL, T. MEINDERS and P. MEINKE 1997 *DFG–Referenzdatensatz A*. Http://www.uni–stuttgart. de/UNIuser/mechb/ARBEIT/refdataA.html.